

# Scattering of charged particles off monopole-antimonopole pairs.

Vicente Vento

*Departamento de Física Teórica - IFIC, Universidad de Valencia - CSIC, E-46100 Burjassot (Valencia), Spain.*

Marco Traini

*INFN - TIFPA, Dipartimento di Fisica, Università degli Studi di Trento,  
Via Sommarive 14, I-38123 Povo (Trento), Italy*

(Dated: September 10, 2019)

The Large Hadron Collider is reaching energies never achieved before allowing the search for exotic particles in the TeV mass range. In a continuing effort to find monopoles we discuss the effect of the magnetic dipole field created by a pair of monopole-antimonopole or monopolium on the successive bunches of charged particles in the beam at LHC.

PACS numbers: 14.80.Hv, 12.90.+b, 12.20.Fv

## I. INTRODUCTION

The theoretical justification for the existence of classical magnetic poles, hereafter called monopoles, is that they add symmetry to Maxwell's equations and explain charge quantization. Dirac showed that the mere existence of a monopole in the universe could offer an explanation of the discrete nature of the electric charge. His analysis leads to the Dirac Quantization Condition (DQC) [1, 2]

$$eg = N/2, \quad N = 1, 2, \dots, \quad (1)$$

where  $e$  is the electron charge,  $g$  the monopole magnetic charge and we use natural units  $\hbar = c = 1 = 4\pi\epsilon_0 = \frac{\mu_0}{4\pi}$ . In Dirac's formulation, monopoles are assumed to exist as point-like particles and quantum mechanical consistency conditions lead to establish the magnitude of their magnetic charge. Monopole physics took a dramatic turn when 't Hooft [3] and Polyakov [4] independently discovered that the SO(3) Georgi-Glashow model [5] inevitably contains monopole solutions [6]. These topological monopoles are impossible to create in particle collisions either because of their huge GUT mass [3, 4] or for their complicated multiparticle structure [7]. In the case of low mass topological solitons they might be created in heavy ion collisions via the Schwinger process [8]. For the purposes of this investigation we will adhere to the Dirac picture of monopoles, i.e., they are elementary point-like particles with magnetic charge  $g$  determined by the Dirac condition Eq.(1) and with unknown mass  $m$  and spin. These monopoles have been a subject of experimental interest since Dirac first proposed them in 1931. Searches for direct monopole production have been performed in most accelerators. The lack of monopole detection has been transformed into a monopole mass lower bounds [9–12]. The present limit is  $m > 400$  GeV [13–18] but experiments at LHC can probe much higher masses. Monopoles may bind to matter and we have studied ways to detect them by means of inverse Rutherford scattering with ions [19, 20].

Since the magnetic charge is conserved monopoles at LHC will be produced predominantly in monopole-antimonopole pairs (or monopolium) [21–24]. This magnetic chargeless pair, given the collision geometry, will produce a magnetic dipole field. We discuss hereafter the scattering of charged particles on a magnetic dipole and will analyze later on how our results affect the particles of the successive bunches at LHC. This development therefore assumes that the monopoles are more massive than the beam particles and therefore their scattering does not affect the dynamics of the formation process.

## II. SCATTERING OF CHARGED PARTICLES BY A MAGNETIC DIPOLE.

Suppose that at LHC a monopole-antimonopole pair is produced by any of the studied mechanisms [8, 21–23, 25]. If the pair is produced close to threshold the pair will move slowly away from each other in the interaction region. These geometry will produce a magnetic dipole in the beamline which affects the particles coming in the successive bunches. We model this scenario as the study of the scattering of a beam of charged particles by a fixed magnetic dipole created by two magnetic charges separated by a fixed distance. We will discuss the peculiarities of monopolium, as a bound state, in Section IV.

The magnetic field of a monopole located at the origin of the coordinate system is given by

$$\vec{B}_g = g \frac{\vec{r}}{r^3}, \quad (2)$$

where  $g$  is the magnetic charge,  $\vec{r}$  the radial vector of coordinates  $(x, y, z)$  and  $r$  the norm of  $\vec{r}$ . Let us construct the magnetic field of a monopole, located at position  $\vec{d} = (0, 0, d)$ , and an antimonopole (located at position  $(0, 0, -d)$ ), where  $d$  is a distance (see Fig. 1),

$$\vec{B}_d = g \frac{\vec{r}_{+d}}{r_{+d}^3} - g \frac{\vec{r}_{-d}}{r_{-d}^3}, \quad (3)$$

where  $\vec{r}_{\pm d} = \vec{r} \mp \vec{d}$  and  $r_{\pm d}$  their norm.

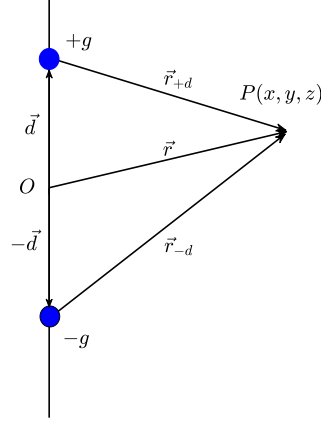


FIG. 1: The magnetic moment configuration discussed in the text.

Let us assume for the moment that  $d \ll r$ . To leading order in  $d$  we obtain the conventional field for a fixed magnetic moment

$$\vec{B}_d = 3 \frac{(\vec{\mathcal{M}} \cdot \vec{r})}{r^5} \vec{r} - \frac{\vec{\mathcal{M}}}{r^3}, \quad (4)$$

where  $\vec{\mathcal{M}} = 2gd\vec{d}$  is the magnetic moment. Note that the magnetic charge field vanishes in the expansion in  $d$  as expected from duality.

Let us study the behavior of the vector potential which is important to determine the interaction between the charged particles of the beam and the magnetic moment. Duality hints us that once the singularities are taken care of the result should resemble the conventional case. The vector potential for a monopole whose magnetic field is Eq.(2) can be written as

$$\vec{A}_g = g \frac{1 - \cos \theta}{r \sin \theta} \hat{\phi} = g \frac{r - z}{r(x^2 + y^2)} (-y, x, 0), \quad (5)$$

where  $\theta \in [0, \pi]$  is the spherical polar angle and  $\hat{\phi} = (-\sin \phi, \cos \phi, 0)$  is the azimuthal unit vector, being  $\phi$  the azimuthal angle. Note that this field is singular for  $\theta = \pi$ , i.e. , this is the famous Dirac string singularity. The vector field generated by the monopole-antimonopole of Fig. 1 is given by

$$\vec{A}_d = g \frac{r_{+d} - z_{+d}}{r_{+d}(x_{+d}^2 + y_{+d}^2)} (-y_{+d}, x_{+d}, 0) - g \frac{r_{-d} - z_{-d}}{r_{-d}(x_{-d}^2 + y_{-d}^2)} (-y_{-d}, x_{-d}, 0), \quad (6)$$

where  $r_{\pm d} = \sqrt{x^2 + y^2 + (z \mp d)^2}$ ,  $x_{\pm d} = x$ ,  $y_{\pm d} = y$  and  $z_{\pm d} = z \mp d$ . If we assume again  $d \ll r$ , and perform a series expansion in  $d$ , the  $d^0$  term does not appear being the  $d^1$  term the first non vanishing term which is

$$\vec{A} = \frac{\vec{\mathcal{M}} \times \vec{r}}{r^3}. \quad (7)$$

This term has the conventional structure and we note that the Dirac string singularities of the monopole and the anti-monopole have disappeared as the magnetic charge term vanishes in the limit.

Minimal coupling applied to the free Schrödinger equation for a spinless particle of charge  $Q$  and mass  $m_A$  leads to an interaction for the magnetic dipole of the form

$$H_{int} = \frac{Q}{2m_A}(\vec{p} \cdot \vec{A} + \vec{A} \cdot \vec{p}) + \frac{Q^2}{2m_A} \vec{A} \cdot \vec{A} = H_{par} + H_{dia}. \quad (8)$$

Note that  $Qg = Z/2$  where  $Ze$  is the charge of the particles in the beam. For the velocities involved in of our physical scenario the diamagnetic term,  $H_{dia}$ , will be small compared to the paramagnetic one and we will neglect it in here. In the chosen gauge  $\nabla \cdot \vec{A} = 0$ , the paramagnetic term can be written as

$$H_{par} = \frac{Q}{m_A} \vec{B} \cdot \vec{L} \quad (9)$$

$\vec{B}$  being  $\nabla \times \vec{A}$  which is equal to

$$H_{par} = \frac{Q}{m_A} \vec{B} \cdot \vec{L} = \frac{Q}{m_A} \frac{\vec{\mathcal{M}} \times \vec{r}}{r^3} = -\vec{\mathcal{M}} \cdot \vec{B}_A \quad (10)$$

where  $\vec{B}_A = Q(\vec{v}_Q \times \vec{r}/r^3)$  is the magnetic field created by the charge in motion. Thus we have shown that within the approximations used the interaction caused by the magnetic field of our magnetic dipole on a charge is the same as the interaction of the magnetic field of the moving charge on the magnetic dipole.

Let us calculate the scattering of charged particles off the magnetic dipole by using the Born approximation which defines the amplitude for the scattering for a spinless charged particle by a magnetic dipole as

$$f(\vec{k} \rightarrow \vec{k}') = -4\pi^2 m_A \langle \vec{k}' | H_{par} | \vec{k} \rangle = -8\pi^2 Zeg \int \frac{d^3 r}{(2\pi)^3} e^{i\vec{k}' \cdot \vec{r}} \left( \frac{\vec{d} \cdot \vec{L}}{r^3} \right) e^{i\vec{k} \cdot \vec{r}}. \quad (11)$$

After some conventional integrations we obtain for the amplitude in the Born approximation from which the cross section becomes

$$\frac{d\sigma}{d\Omega}(\theta)|_{nr} = Z^2 d^2 \cot^2 \theta / 2. \quad (12)$$

The expansion of the vector potential in  $d$  is described by a series of the form  $A_1(x, y, z)d + A_2(x, y, z)d^3 + A_3(x, y, z)d^5 + \dots$ . Therefore by dimensional arguments the scattering amplitude will appear as an expansion in  $f_1(\theta)d + f_2(\theta)(kd)^2d + f_3(\theta)(kd)^4d + \dots$ . Thus this approximation is only valid for small values of  $kd$ . However, it might happen, that the series sums to a bounded function and then one can find resonable estimates for large  $kd$ . We proceed to attempt the sum of the whole series.

We apply the Born approximation directly to the full potential in  $A_d$  as in

$$f(\vec{k} \rightarrow \vec{k}') = -4i\pi^2 Zeg \int \frac{d^3 r}{(2\pi)^3} e^{-i\vec{k} \cdot \vec{r}} \vec{k} \cdot \vec{A}_d e^{-i\vec{k}' \cdot \vec{r}}. \quad (13)$$

In the first term of  $\vec{A}_d$  we change the variable  $\vec{r} - \vec{d}$  by  $\vec{r}$  and we get for the integral

$$ke^{-i\vec{q}\cdot\vec{d}} \int \frac{d^3r}{(2\pi)^3} e^{-i\vec{q}\cdot\vec{r}} \frac{x}{r(r+z)}, \quad (14)$$

where we have taken  $\vec{k} = k(0, 1, 0)$  and  $\vec{q} = \vec{k}' - \vec{k}$ . In this way we have eliminated the  $\vec{d}$  dependence from the integral. We can do the same trick in the second term by changing the variable  $\vec{r} + \vec{d}$  by  $\vec{r}$ .

$$ke^{+i\vec{q}\cdot\vec{d}} \int \frac{d^3r}{(2\pi)^3} e^{-i\vec{q}\cdot\vec{r}} \frac{x}{r(r+z)}, \quad (15)$$

Let

$$f(q) = \int \frac{d^3r}{(2\pi)^3} e^{-i\vec{q}\cdot\vec{r}} \frac{x}{r(r+z)} \quad (16)$$

then

$$f(\vec{k} \rightarrow \vec{k}') = -\frac{Zeg}{\pi} k f(q) \sin \vec{q} \cdot \vec{d}. \quad (17)$$

The integral  $f(q)$  is quite complex however we know that in the limit  $d \rightarrow 0$  we should get our previous result Eq.(12) therefore,

$$f(q) = \frac{i\pi}{k^2 \sin^2 \theta/2} = \frac{i\pi}{q^2}. \quad (18)$$

The cross section for  $d$  finite becomes

$$\frac{d\sigma}{d\Omega}|_{nr} = \frac{Z^2}{4k^2} \frac{\sin^2(kd \sin \theta)}{\sin^4(\theta/2)}. \quad (19)$$

By assuming that the scattered wave is much smaller than the incoming wave we estimate the validity of the Born approximation as given by

$$\left| \frac{m_A Z}{k} \right| < 1. \quad (20)$$

This limits the energy of the beam to  $k \gg m_A Z = m_A (GeV/nucleon)$ , satisfied certainly at LHC, but we must study some relativistic corrections.

Let us start by studying a beam of spinless particles. The corresponding Klein-Gordon equation reads

$$((E - A_0)^2 - (\vec{p} - Q\vec{A})^2)\Phi = m^2\Phi \quad (21)$$

Taking  $A_0 = 0$ , considering only the paramagnetic interaction term and choosing the gauge where  $\vec{\nabla} \cdot \vec{A} = 0$  we get

$$(\nabla^2 + k^2)\Phi = 2Q(\vec{B} \cdot \vec{L})\Phi, \quad (22)$$

where  $k^2 = E^2 - m^2$ . This equation has to be compared with the Schrödinger equation

$$(\nabla^2 + 2mE)\Phi = 2Q(\vec{B} \cdot \vec{L})\Phi. \quad (23)$$

Thus relativity is implemented just by substituting the non relativistic momentum  $k = \sqrt{2mE}$  by the relativistic one  $k = \sqrt{E^2 - m^2}$ . Therefore, the structure of the cross section in the Born approximation does not change,

$$\frac{d\sigma}{d\Omega}(\theta) = \frac{d\sigma}{d\Omega}(\theta)|_{nr}. \quad (24)$$

Let us assume now that we have a beam of unpolarized spin 1/2 particles. Using the conventional notation the Dirac equation for our problem becomes

$$(E + \vec{\alpha} \cdot (\vec{p} - Q\vec{A}) + m\beta)\Psi = 0. \quad (25)$$

We next multiply by  $E - \vec{\alpha} \cdot (\vec{p} - Q\vec{A}) - m\beta$  [26, 27], and we obtain

$$(\nabla^2 + k^2)\Psi = 2Q(\vec{B} \cdot \vec{L})\Psi, \quad (26)$$

which leads to the same equation as before for each component using the relativistic momentum. Thus again the structure does not change,

Before ending this section it must be noted that we are performing the calculation in the most favorable situation in which the dipole is perpendicular to the beam.

### III. SCATTERING OF CHARGED PARTICLES ON A PAIR MONOPOLE-ANTIMONOPOLE

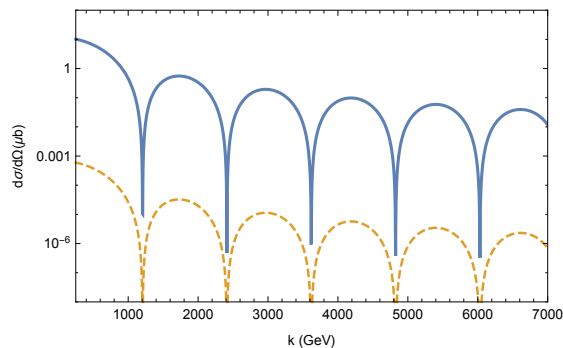


FIG. 2: We show the elastic proton-magnetic dipole scattering differential cross section in microbarns ( $\mu\text{b}$ ) for a proton beam. In order to see the structure of the cross section we have chosen  $d = 0.003$  fm. We show two limiting angular dependencies for  $10^0$  (full) and  $170^0$  (dashed).

Let us use the above study for LHC physics. Imagine that monopole-antimonopole pairs are created in the collisions [21–23]. Some of those pairs annihilate into photons and some of them escape the interaction region. The annihilation cross sections has been studied for some time [22, 29, 30]. Those monopoles which escape might be detected directly or bind to matter and methods for detection have been devised [15, 20, 25, 31]. We are here interested in discussing what happens while the pairs are escaping the interaction region because this effect might help disentangle the monopole from other exotic particles. A pair of opposite magnetic charges will create a magnetic dipole field as we have shown in the previous section from which the particles of the beam will scatter. We study next what happens with proton and ion beams at LHC with the maximum planned beam energy 7 TeV and maximum luminosity  $2 \cdot 10^{34} \text{cm}^{-2} \text{s}^{-1}$ .

We study proton beams first. Using Eq.(19) with relativistic momenta we plot in Fig. 2 the shape of the cross section as a function of momentum for two angles  $10^0$  and  $170^0$ . For drawing purposes we choose a value of  $d \sim 0.003$  fm to show the momentum dependence of the cross section with its pics and valleys.

In order to get some realistic estimates for detection we have to fix several scales. The first scale to fix is  $d$ . The minimum possible value for  $d$  is twice the classical radius of the monopole ( $\sim 2g^2/m$ ) which for a monopole of mass 500 GeV is  $\sim 0.03$  fm. Since for LHC  $k \sim 7$  TeV in this case  $kd \sim 10^3$  and therefore the oscillations in the amplitude are extremely rapid. It is therefore an excellent approximation to take for an average cross section the envelop of the curve divided by  $\sqrt{2}$ . Thus our cross section becomes  $d$  independent for all interesting values of  $d$ .

The next parameter we need to determine is the duration of the collision. This parameter together with the luminosity of LHC,  $2 \cdot 10^{34} \text{cm}^{-2} \text{s}^{-1}$ , will determine the number of photons scattered by each pair. To determine that number we need to know the maximum separation at which the dipole is still active and the velocity of separation from the impact point. We will use for the separation distance two values: i) the width of the bunch  $\sim 16 \mu\text{m}$ , and ii) the diameter of the beam pipe, 45 mm. The average effect will be between these two values  $0.8 \cdot 10^{-13} \text{s} < \beta t < 1.5 \cdot 10^{-10} \text{s}$ .

In our plots we take for  $\beta$  the value 0.01, noting that  $\beta$  enters the equation as  $\sim 1/\beta$ , thus a rescaling of our results is trivial.

Finally we need to know the number of pairs produced in the collisions. We used the production cross section for spin 0 monopoles [2] calculated using the techniques of refs. [21–23].

Let us discuss first monopoles of 500 GeV mass with Dirac coupling  $g$  given by the quantization condition Eq.(1). The cross section for the pairs produced is  $\sim 1000$  pb<sup>1</sup>.

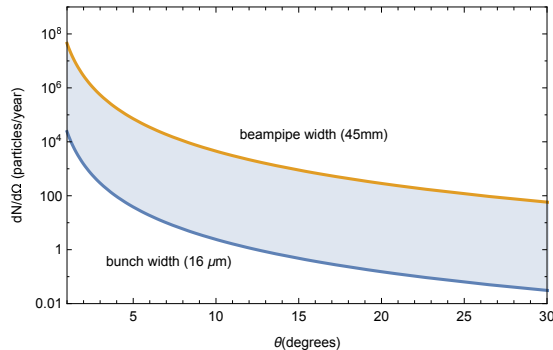


FIG. 3: We show the average number of protons scattered in one year from a 7 TeV proton beam at an LHC luminosity of  $2 \cdot 10^{34} \text{ cm}^{-2} \text{ s}^{-1}$  by a monopole-antimonopole separating at velocity  $\beta = 0.01$  as a function of scattering angle for the geometry that maximises the cross section. The upper curve corresponds to a time scale associated with the beampipe diameter while the lower curve corresponds to the time scale associated with the width of the proton bunch.

With these scales fixed we calculate the number of protons scattered in one year assuming that the elements of the pair separate with a velocity  $\beta = 0.01$ . The result of the calculation is shown in Fig. 3. The upper curve corresponds to a time scale associated with the beampipe diameter while the lower curve to the time scale associated with the bunch width. The result corresponds to a typical electromagnetic interaction where the forward direction is favored, but where backward scatterings are an important characteristic. Thus from an experimental point of view it is the non-forward directions which characterize better the monopoles. We see that detection in the near-forward direction is possible and the scenario is specially suited for the big detectors ATLAS, CMS and LHCb. These observations are complementary to direct detection and the annihilation of monopole-antimonopole pairs into photons. Direct detection might not differentiate monopoles from other exotics and annihilation produces broad bumps which are not very characteristic [22, 29, 30]. However, together with the observation of non-forward protons of beam energy they become a clear identification of monopole production.

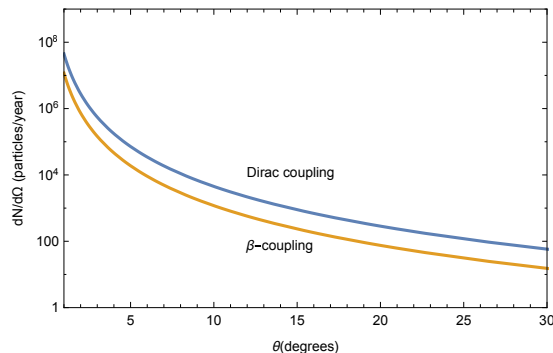


FIG. 4: We compare the results obtained previously for the number of protons scattered with Dirac coupling with those of  $\beta$ -coupling for 500 GeV monopole mass. We have taken for this comparison the time scale associated with the beampipe diameter.

<sup>1</sup> We are working with Dirac monopoles of charge  $g$  thus the cross section is greater than that shown in refs.[21–23] where they use  $\beta$ -coupling.

The  $\beta$ -coupling schemes used in many calculation [21, 22] leads to production cross sections which are smaller and therefore to a smaller number of protons scattered as shown in Fig. 4. The monopole-antimonopole production cross section decreases rapidly with the monopole mass [21–23] and so will the number of scattered protons. We show these results in Fig. 5 for Dirac coupling. Thus for larger monopole masses the dipole effect becomes more and more difficult to detect. By looking at the dipole cross section Eq.(19) one would think that detection would increase for lower momenta, but the production cross section of pairs also diminishes for lower momenta. We can see that in our model the decrease in production dominates over the increase in dipole scattering in the right side of Fig.5. However, the cancellation between the two is model dependent and therefore no clear conclusion can be established, except that the difference in cross sections for different momenta is small once we are well above threshold, i.e. there is little momentum dependence.

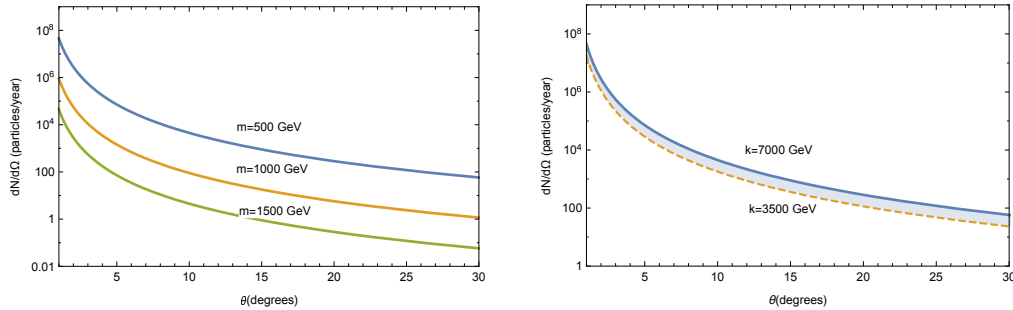


FIG. 5: We show the average number of protons scattered in one year from proton beams at an LHC luminosity of  $2 \cdot 10^{34} \text{ cm}^{-2} \text{ s}^{-1}$  by a monopole-antimonopole separating at velocity  $\beta = 0.01$  as a function of scattering angle for the geometry that maximises the cross section. The figure on the left has been calculated for a 7 TeV beam for three monopole masses: 500, 1000, 1500 GeV; the figure on the right shows the number of protons scattered for two proton beams at 3.5 TeV and 7 TeV and monopole mass 500 GeV.

Let us discuss next heavy ion scenarios by studying  $^{208}\text{Pb}^{82+}$  beams. In Fig. 6 we show the structure of the cross section for a small  $d = 0.0003 \text{ fm}$ . In order to get estimates we fix the scales again. The dipole distance  $d$  becomes again irrelevant for this large momenta since the minimum range is determined by the classical radius of the monopole. This makes the oscillations even tighter and we resort again to the average cross section, i.e. we use the envelop of the pics divided by  $\sqrt{2}$ . The effective duration of the interaction is calculated as before, namely as the time that takes the pair to get out of the bunch or to get out of the beampipe. Since the bunches have the same size as for the proton and the beampipes about the same size in all detectors we use the same time scales. We take the same escape velocity of the ions  $\beta = 0.01$ . Since the collision takes place in an extreme relativistic scenario we will approximate the lead nucleus by a flat pancake, assume central collisions and thus the production cross section for monopole-antimonopole pairs can be approximated by  $Z^2\sigma(pp)$ , noting that photon fusion is the dominant production mechanism and that the neutrons do not contribute to production. Unluckily the luminosity for ions at LHC is much smaller,  $10^{27} \text{ cm}^{-2} \text{ s}^{-1}$ . This factor proves to be dramatic in not allowing detection. We show in Fig. 7 (left) the average number of particles scattered per year for a  $^{208}\text{Pb}^{82+}$  beam. It is clear that with the present LHC luminosity for lead the possibility of measuring the dipole effect with lead ions is out of question. In order to see a signature for the MoEDAL detector the luminosity has to be increased minimally by  $10^4$ . In Fig.7 (right) we show the results for this luminosity. Detection is difficult but possible in the slightly off-forward direction.

We can see in Fig. 8 a similar behavior as shown previously for protons, namely that the cross section for 1.28 TeV/nucleon is slightly smaller than that associated to 2.76 TeV/nucleon for the wishful luminosity. Again there is a strong cancellation between the production cross section and dipole scattering cross section. The shown result is model dependent but dependence on momentum, once we are well above threshold, is small.

We can summarize the results of our investigation by concluding that the dipole effect of an monopole-antimonopole pair may be detectable at LHC if monopole masses do not exceed 1000 GeV with available proton beams and reachable luminosities. With ion beams and present luminosities, detection is not feasible. The signal for the existence of the pair is clear, one should look for protons at beam energies in the off-forward beam directions.

#### IV. SCATTERING OFF MONOPOLIUM

Monopolium is a boundstate of monopole-antimonopole. It cannot have a permanent dipole moment. However, in the vicinity of a magnetic field it can get an induced magnetic dipole moment through its response to the external

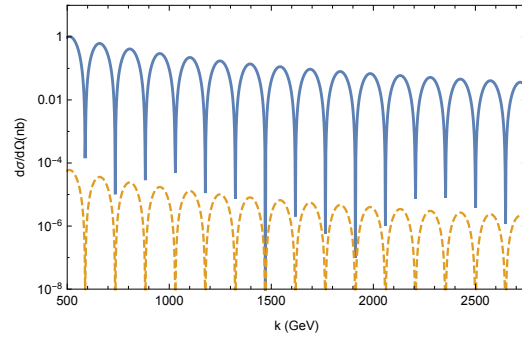


FIG. 6: We show the elastic scattering differential cross section in nanobarns (nb) for a  $^{208}\text{Pb}^{82+}$  beam. In order to see the structure of the cross section we have chosen  $d = 0.0003$  fm. We show two limiting angular dependencies for  $10^0$  (full) and  $170^0$  (dashed).

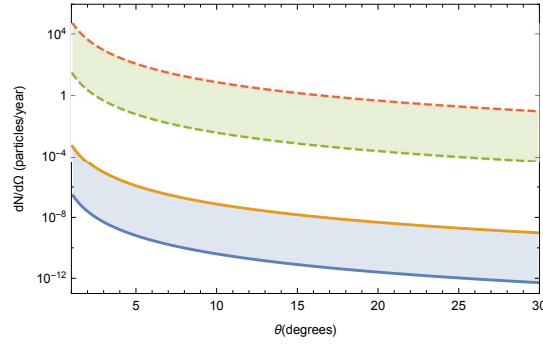


FIG. 7: The figure shows the average number of ions scattered by a monopole-antimonopole pair for a 2.76 TeV/nucleon  $^{208}\text{Pb}^{82+}$  beam, with  $\beta = 0.01$  and luminosity  $10^{27} \text{ cm}^{-2} \text{ s}^{-1}$  (solid) and with  $\beta = 0.01$  and luminosity  $10^{31} \text{ cm}^{-2} \text{ s}^{-1}$  (dashed). The upper curve of each band corresponds to the beampipe diameter time scale while the lower curve to the bunch width time scale

magnetic field. In quantum mechanics the magnetic polarizability  $\alpha$  is connected to the change of the energy levels of the system caused by the external field. The general framework to evaluate these changes is the (stationary) perturbation theory applied to the total Hamiltonian which, in the case of a Monopolum immersed in a static (and

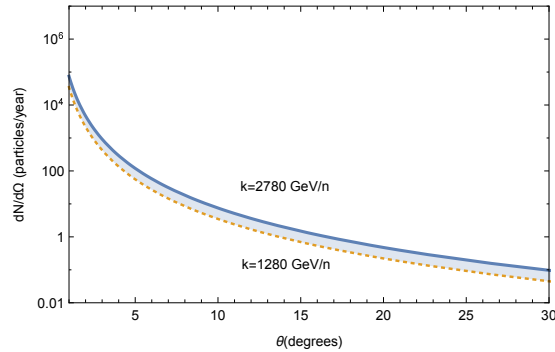


FIG. 8: We show the average number of ions scattered by a monopole-antimonopole pair for a 2.76 TeV/nucleon  $^{208}\text{Pb}^{82+}$  beam and 1.38 2.76 TeV/nucleon  $^{208}\text{Pb}^{82+}$  beam. We use  $\beta = 0.01$  and luminosity  $10^{31} \text{ cm}^{-2} \text{ s}^{-1}$ .



uniform) magnetic field  $\vec{B}$ , can be written

$$\begin{aligned} H(\vec{B}) &= H_0 + H'(\vec{B}) = H_0 - \vec{\mathcal{M}} \cdot \vec{B} \\ &= \frac{\vec{p}^2}{2\mu} + V_{M\bar{M}}(r) - \mathcal{M} B, \end{aligned} \quad (27)$$

where  $\mu = m/2$  is the reduced mass of the monopole,  $V_{M\bar{M}}$  the potential energy associated to the monopole - antimonopole interaction within a non-relativistic framework and  $\vec{\mathcal{M}}$  the magnetic dipole induced in the system. The (negative) lower order correction to the ground state energy of the system is quadratic in the perturbative field and defines the magnetic (paramagnetic) susceptibility  $\alpha_M$

$$\lim_{B \rightarrow 0} \langle \vec{B} | H_0 + H'(\vec{B}) | \vec{B} \rangle = E_0 - \frac{1}{2} \alpha_M \vec{B}^2, \quad (28)$$

where  $|\vec{B}\rangle$  is the ground state of  $H(\vec{B})$ ,  $E_0$  the ground state energy value of the unperturbed Hamiltonian  $H_0$  and  $B = |\vec{B}|$ . The magnetic dipole operator  $\vec{\mathcal{M}}$  is inferred by the duality from the analogous electric dipole operator:

$$\vec{D} = e\vec{r} \rightarrow \vec{\mathcal{M}} = g\vec{r} \quad (29)$$

where  $\vec{r}$  is the relative position of the monopole and antimonopole.

The susceptibility  $\alpha_M$  can be equivalently defined from the induced magnetic moment as in the classical case, namely

$$\alpha_M = \lim_{B \rightarrow 0} \frac{\langle \vec{B} | \mathcal{M} | \vec{B} \rangle}{B}. \quad (30)$$

Both Eqs. (28) and (30) lead to the well know perturbative expression (recall that  $\langle 0 | \mathcal{M} | 0 \rangle = 0$  because of parity invariance)

$$\alpha_M = 2 \sum_{n \neq 0}^{\infty} \frac{|\langle n | \mathcal{M} | 0 \rangle|^2}{E_n - E_0} = 2m_{-1}(\mathcal{M}), \quad (31)$$

which relates the polarizability  $\alpha_M$  to the inverse energy-weighted sum rule  $m_{-1}$ . Because of the rigorous bounds among sum rules one can estimate  $m_{-1}$  through a lower bound

$$m_{-1}(\mathcal{M}) \geq \frac{m_0^2(\mathcal{M})}{m_1(\mathcal{M})} \quad (32)$$

with

$$m_0(\mathcal{M}) = \sum_{n=0}^{\infty} |\langle n | \mathcal{M} | 0 \rangle|^2, \quad (33)$$

$$m_1(\mathcal{M}) = \sum_{n=0}^{\infty} (E_n - E_0) |\langle n | \mathcal{M} | 0 \rangle|^2. \quad (34)$$

Thus to get an estimate for the polarizability one has to calculate the first few sum rules for the magnetic dipole operator (29):

$$\mathcal{O} \equiv \mathcal{M} = g z, \quad (35)$$

where  $z$  is the relative distance of monopole and anti-monopole in the direction of the external field. Since monopolum is a two-body system the calculation of the sum rules can be performed rather easily not only for the odd moments which depend on commutators, but for the even moments also, although they require the evaluation of anticommutators [32].

i)  $m_0$  gives the total integrated response function

$$m_0(\mathcal{M}) = \frac{1}{2} \langle 0 | \{ \mathcal{M}, \mathcal{M} \} | 0 \rangle = g^2 \frac{1}{3} \langle 0 | \vec{r}^2 | 0 \rangle, \quad (36)$$

and is related to the rms radius of the monopolum;

ii)  $m_1$  leads to

$$\begin{aligned} m_1(\mathcal{M}) &= \frac{1}{2} \langle 0 | [\mathcal{M}, [H_0, \mathcal{M}]] | 0 \rangle = \\ &= g^2 \frac{\hbar^2}{2\mu}; \end{aligned} \quad (37)$$

The simplicity of the previous commutator is basically due to the fact that the commonly used monopole-antimonopole potentials,  $V_{M\overline{M}}$ , commute with the magnetic dipole operator (29).

Lower and upper bounds to the magnetic susceptibility can be found. The so called Feynman bound is given by [33, 34],

$$\alpha_M \geq \frac{2m_0^2}{m_1}. \quad (38)$$

We make here the assumption that the previous lower bound can reasonably approximate the magnetic susceptibility for monopole as established in other contexts [32–34], thus

$$\alpha_M \approx 2 \frac{m_0^2(\mathcal{M})}{m_1(\mathcal{M})} = \frac{4}{9} \frac{\mu c^2}{(\hbar c)^2} g^2 [\langle r^2 \rangle]^2, \quad (39)$$

where  $\langle r^2 \rangle$  is the mean square radius of the monopole system.

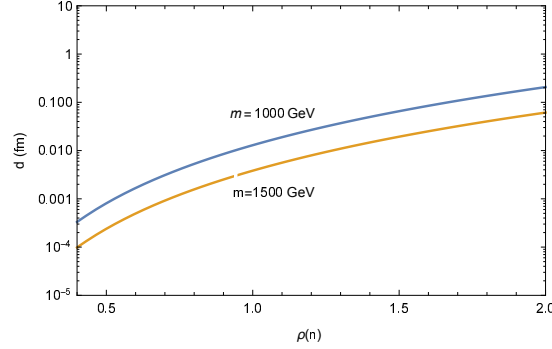


FIG. 9: We plot the stiffness distance of monopole as a function of the size parameter for two values of the monopole mass.

Let us describe the physical scenario for detection of monopole. We assume that monopole is produced at LHC at 14 TeV fundamentally by photon fusion by the reaction

$$p + p \rightarrow p + p + M. \quad (40)$$

Let us assume that monopole is produced near threshold with a mass below 2000 GeV. The time scale of the process is dominated by the lifetime of monopole  $t \sim \frac{1}{\Gamma} \sim \frac{1}{10} \text{ GeV}^{-1}$ . The protons travel close to the speed of light and therefore the distance scales are  $\sim 0.02 \text{ fm}$ . The magnetic field created by the moving protons deforms monopole and gives it a magnetic moment,

$$\vec{\mathcal{M}} = \alpha_M \vec{B} = 2g\vec{d}, \quad (41)$$

where we equate the induced magnetic moment to that of an effective dipole as described in previous sections.  $d$  is a measure of the stiffness of monopole. In this way we will apply the formalism developed in the previous sections to this effective magnetic moment. Our goal is to estimate  $\alpha_M$  and  $B$  to get  $d$  and then we apply the scattering formalism of previous sections.

To calculate  $\alpha_M$  we need to have a model for monopole, i.e. an interaction potential. There are several models in the literature [29, 35] but for the purpose of the present investigation, where a precise value of  $d$  is not relevant as long as  $kd$  is large, the approximation to the potential of Schiff and Goebel [35]

$$V(r) = -g^2 \frac{1 - \exp(-2r/r_0)}{r}, \quad (42)$$

used in ref.[28] will be sufficient. The approximation consists in substituting the true wave functions by Coulomb wave functions of high  $n$ . For each  $r_0$  a different value of large  $n$  will be best suited. We used the equation

$$\rho = 48\alpha^2 n^2 \quad (43)$$

being  $\rho = r_M/r_{classical}$ , where  $r_M$  is the expectation value of  $r$  in the  $(n, 0)$  Coulomb state, and  $\alpha$  the electromagnetic fine structure constant  $\sim \frac{1}{137}$  to parametrize all expectation values in terms of  $\rho$ , which we allow to be continuous. For example the binding energy becomes

$$M = m(2 - \frac{3}{4\rho}), \quad (44)$$

a continuous function in terms of  $\rho$  which covers the interval  $[0, 2m]$ . In this approximation all the moments can be determined analytically

$$m_0 = \frac{1}{864} \frac{\rho(5\rho + 48\alpha^2)}{m^2},$$

$$m_1 = \frac{1}{4\alpha m},$$

The magnetic susceptibility obtained from the Feynman estimate Eq.(38) becomes

$$\alpha_M = \frac{1}{93312} \frac{\rho^2(5\rho + 48\alpha^2)^2}{m^3\alpha^5}. \quad (45)$$

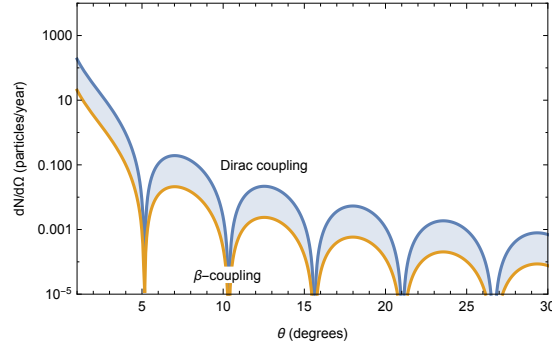


FIG. 10: We plot the number of protons scattered as a function of scattering angle in the strong binding limit  $m = 1000$  GeV  $\rho = 0.5$ .

Let us now estimate the magnetic field acting on monopolum. We are assuming that monopolum is moving slowly as compared to the protons ( $\beta_M \sim 0.01$ ), therefore it is static in the time scale of the problem. The proton which creates the magnetic field is moving very fast,  $\beta_p \sim 1$ . The time scale of the problem is determined by the lifetime of monopolum which leads to an effective radius of  $R \sim 0.02$  fm, thus

$$B \sim \frac{2e\beta_p}{R^2} \sim 8.5 \text{ GeV}^2. \quad (46)$$

The effective distance, Eq. (41) becomes

$$d = 0.15 \left( \frac{\alpha_M}{\text{GeV}^3} \right) \text{ fm} \quad (47)$$

In order to perform the calculation we require the monopolum production cross section. To do so we have used the formalism and computational programs of [28] with updated pdfs.

In Fig. 9 we plot  $d$  as a function of size parameter for  $m = 1000, 1500$  GeV. Since the minimum value of the  $d$  is  $\sim 0.001$  fm even for the large momenta of the protons oscillations are visible in the plot for strong bound monopolum ( $\rho \sim 0.5$ ) as can be seen in Fig. 10, where we also show the result for  $\beta$ -coupling which leads to a smaller production

cross section. In order to calculate the protons scattered by monopolium we use for monopolium also the approximate average value as described before. In this way comparison with the results of previous sections is more transparent.

In the next Figs. 11 we show the dependence of the number of protons scattered per year as a function of scattering angle for different values of the size parameter, monopole masses and proton momenta. The figure on the left shows that the strong binding scenario might allow detection, for monopolia with a mass below 1000 GeV, while observations in the weak binding scenario are hopeless. The figure in the center shows that as we increase the monopole mass for a fixed  $\rho$  the cross sections becomes smaller and observability is reduced. In the figure to the right we analyze the momentum dependence by comparing the results for 3.5 TeV protons and 7 TeV protons. Again we discover the cancellation observed earlier between the production and the dipole scattering cross section as we change momenta. The important result is that experiments do not seem to be very much model dependent on kinematics as long as we are well above production threshold.

To summarize, we stress that the analysis for monopolium depends strongly on the details of the dynamics. Different monopole-antimonopole potentials might lead to different results. In particular it depends very strongly on the binding energy and the decay width. Large binding energies and small widths will increase observability. Given the neutral nature of monopolium this type of experiment would be ideal for its detection, however the apparent short lifetime of monopolium and the reachable luminosities at LHC make observability difficult.

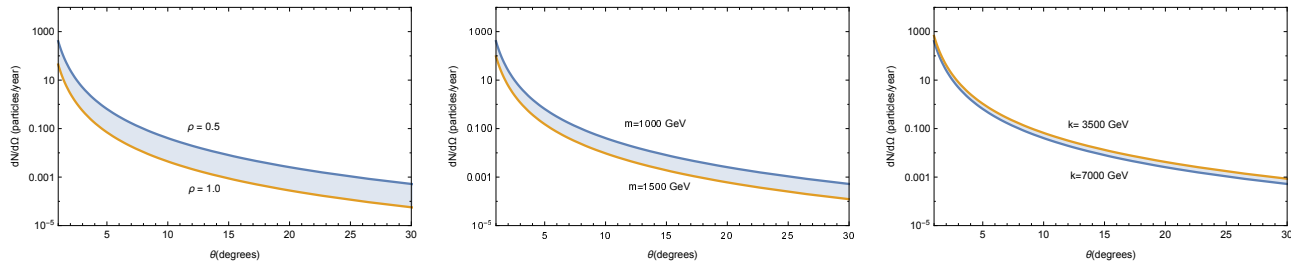


FIG. 11: We show the average number of protons scattered in one year from a proton beam at an LHC luminosity of  $2 \cdot 10^{34} \text{ cm}^{-2} \text{ s}^{-1}$  by monopolium moving at velocity  $\beta = 0.01$  as a function of scattering angle for the geometry that maximises the cross section. Left: for  $k=7$  TeV,  $m=1000$  GeV and different size parameters; center: for  $\rho = 0.5$ ,  $k=7$  TeV and different masses; right: for  $\rho = 0.5$ ,  $m=1000$  GeV and the momenta shown.

## V. CONCLUDING REMARKS

In previous work we studied ways to detect Dirac monopoles bound in matter by means of proton and ion beams [20]. We also studied the possibility of finding monopoles not free but in bound pairs of monopole-antimonopole, the so called monopolium [22, 28]. Monopolium has lower mass than a pair of monopole-antimonopole and also annihilates into photons [29, 30] but because it is neutral it is difficult to detect directly. In this paper we pursue some investigations to detect monopoles in LHC besides direct detection and their decay properties. We study the distortion produced in the beam by their permanent or induced magnetic dipole moment to characterize detectability. We have modelled the interaction by a fixed magnetic dipole made by two magnetic charges  $g$  and  $-g$  separated by a distance  $d$ . We have studied how this effective magnetic dipole interacts with a beam of charged particles. The main result is that the beam particles will be deflected and therefore particles with beam energy will appear in off-forward directions. We have shown that monopole-antimonopole pairs lead to a sizeable effect with the proton beams at LHC and thus the effect is suitable for detection in ATLAS, CMS and LHCb. However, present heavy ion luminosities do not allow detection which makes the scenario not useful for MoEDAL. In the case of monopolium the strong coupling limit might lead to near forward protons, a scenario which could help detect this neutral particle, however this result is model dependent and the signatures are small appearing only for small angles.

To conclude monopoles can be detected directly or by the decay of monopole-antimonopole pairs into photons. Monopolium can be detected by its decay into photons. We have shown that detecting beam particles at beam energy in non-forward directions becomes an additional tool for monopole and monopolium detection.

## Acknowledgement

M.T. thanks the Department of Theoretical Physics of the University of Valencia for a Visiting Professor grant and for the warm and friendly hospitality. This work was supported in part by the MICINN and UE Feder under contract FPA2016-77177-C2-1-P and SEV-2014-0398.

- 
- [1] P. A. M. Dirac, Proc. Roy. Soc. Lond. A **133** (1931) 60.
  - [2] P. A. M. Dirac, Phys. Rev. **74** (1948) 817. doi:10.1103/PhysRev.74.817
  - [3] G. 't Hooft, Nucl. Phys. B **79** (1974) 276.
  - [4] A. M. Polyakov, JETP Lett. **20** (1974) 194 [Pisma Zh. Eksp. Teor. Fiz. **20** (1974) 430].
  - [5] H. Georgi and S. L. Glashow, Phys. Rev. Lett. **28** (1972) 1494.
  - [6] Y. M. Shnir, "Magnetic monopoles," Berlin, Germany: Springer (2005) 532 p
  - [7] A. K. Drukier and S. Nussinov, Phys. Rev. Lett. **49** (1982) 102. doi:10.1103/PhysRevLett.49.102
  - [8] O. Gould and A. Rajantie, Phys. Rev. Lett. **119** (2017) no.24, 241601 doi:10.1103/PhysRevLett.119.241601 [arXiv:1705.07052 [hep-ph]].
  - [9] A. Abulencia *et al.* [CDF Collaboration], Phys. Rev. Lett. **96** (2006) 201801 [hep-ex/0509015].
  - [10] M. Fairbairn, A. C. Kraan, D. A. Milstead, T. Sjostrand, P. Z. Skands and T. Sloan, Phys. Rept. **438** (2007) 1 [hep-ph/0611040].
  - [11] G. Abbiendi *et al.* [OPAL Collaboration], Phys. Lett. B **663** (2008) 37 [arXiv:0707.0404 [hep-ex]].
  - [12] G. Aad *et al.* [ATLAS Collaboration], Phys. Rev. Lett. **109** (2012) 261803 [arXiv:1207.6411 [hep-ex]].
  - [13] G. Aad *et al.* [ATLAS Collaboration], Phys. Rev. D **93** (2016) no.5, 052009 doi:10.1103/PhysRevD.93.052009 [arXiv:1509.08059 [hep-ex]].
  - [14] T. Lenz, PoS LHCP **2016** (2016) 104 [arXiv:1609.08369 [hep-ex]].
  - [15] B. Acharya *et al.* [MoEDAL Collaboration], Int. J. Mod. Phys. A **29** (2014) 1430050 doi:10.1142/S0217751X14300506 [arXiv:1405.7662 [hep-ph]].
  - [16] B. Acharya *et al.* [MoEDAL Collaboration], JHEP **1608** (2016) 067 doi:10.1007/JHEP08(2016)067 [arXiv:1604.06645 [hep-ex]].
  - [17] B. Acharya *et al.* [MoEDAL Collaboration], Phys. Rev. Lett. **118** (2017) no.6, 061801 doi:10.1103/PhysRevLett.118.061801 [arXiv:1611.06817 [hep-ex]].
  - [18] B. Acharya *et al.* [MoEDAL Collaboration], [arXiv:1712.09849 [hep-ex]].
  - [19] Y. Kazama, C. N. Yang and A. S. Goldhaber Phys. Rev. D **15** (1977) 2287. doi:10.1103/PhysRevD.15.2287
  - [20] V. Vento, Universe **4** (2018) no.11, 117. doi:10.3390/universe4110117
  - [21] T. Dougall and S. D. Wick, Eur. Phys. J. A **39** (2009) 213 doi:10.1140/epja/i2008-10701-8 [arXiv:0706.1042 [hep-ph]].
  - [22] L. N. Epele, H. Fanchiotti, C. A. G. Canal, V. A. Mitsou and V. Vento, Eur. Phys. J. Plus **127** (2012) 60 doi:10.1140/epjp/i2012-12060-8 [arXiv:1205.6120 [hep-ph]].
  - [23] S. Baines, N. E. Mavromatos, V. A. Mitsou, J. L. Pinfold and A. Santra, Eur. Phys. J. C **78** (2018) no.11, 966 Erratum: [Eur. Phys. J. C **79** (2019) no.2, 166] doi:10.1140/epjc/s10052-018-6440-6, 10.1140/epjc/s10052-019-6678-7 [arXiv:1808.08942 [hep-ph]].
  - [24] V. Vento, Int. J. Mod. Phys. A **23** (2008) 4023 doi:10.1142/S0217751X08041669 [arXiv:0709.0470 [astro-ph]].
  - [25] K. A. Milton, Rept. Prog. Phys. **69** (2006) 1637 doi:10.1088/0034-4885/69/6/R02 [hep-ex/0602040].
  - [26] M. E. Rose, Phys. Rev. **73** (1948) 279. doi:10.1103/PhysRev.73.279
  - [27] G. Parzen Phys. Rev. **80** (1950) 261 doi:10.1103/PhysRev.80.261
  - [28] L. N. Epele, H. Fanchiotti, C. A. Garcia Canal and V. Vento, Eur. Phys. J. C **56** (2008) 87 doi:10.1140/epjc/s10052-008-0628-0 [hep-ph/0701133].
  - [29] N. D. Barrie, A. Sugamoto and K. Yamashita, PTEP **2016** (2016) no.11, 113B02 doi:10.1093/ptep/ptw155 [arXiv:1607.03987 [hep-ph]].
  - [30] H. Fanchiotti, C. A. Garcia Canal and V. Vento, Int. J. Mod. Phys. A **32** (2017) no.35, 1750202 doi:10.1142/S0217751X17502025 [arXiv:1703.06649 [hep-ph]].
  - [31] G. Giacomelli, L. Patrizii and Z. Sahnoun, doi:10.1142/9789814340861-0039 arXiv:1105.2724 [hep-ex].
  - [32] Jackiw R 1967 Phys. Rev. **157** 1220; Leonardi R and Rosa-Clot M 1971 Rivista Nuovo Cimento **1** 1; Bohigas O, Lane A M and Martorell J 1979 Phys. Rep. **51** 267; Lipparini E and Stringari S 1989 Phys. Rep. **175** 103; Orlandini G and Traini M 1991 Rep. Prog. Phys. **54** 257
  - [33] Traini M and Leonardi L 1994 Phys. Lett. B **334** 7
  - [34] Traini M Eur. J. Phys. **17** (1996) 30.
  - [35] L.I. Schiff, Phys. Rev. **160** 1257; C.J. Goebel, Quanta, In: Essays in Theoretical Physics, ed. by P.G.O. Freund, C.J. Goebel, Y. Nambu (University of Chicago Press, 1970)